

Zeitschrift: Schweizerische mineralogische und petrographische Mitteilungen =
Bulletin suisse de minéralogie et pétrographie

Band: 56 (1976)

Heft: 1

Artikel: Plagioclase determination through measurement of the extinction
angles in sections normal to (010) and (001)

Autor: Bruni, Paolo

DOI: <https://doi.org/10.5169/seals-43673>

Nutzungsbedingungen

Die ETH-Bibliothek ist die Anbieterin der digitalisierten Zeitschriften. Sie besitzt keine Urheberrechte an den Zeitschriften und ist nicht verantwortlich für deren Inhalte. Die Rechte liegen in der Regel bei den Herausgebern beziehungsweise den externen Rechteinhabern. [Siehe Rechtliche Hinweise.](#)

Conditions d'utilisation

L'ETH Library est le fournisseur des revues numérisées. Elle ne détient aucun droit d'auteur sur les revues et n'est pas responsable de leur contenu. En règle générale, les droits sont détenus par les éditeurs ou les détenteurs de droits externes. [Voir Informations légales.](#)

Terms of use

The ETH Library is the provider of the digitised journals. It does not own any copyrights to the journals and is not responsible for their content. The rights usually lie with the publishers or the external rights holders. [See Legal notice.](#)

Download PDF: 18.03.2025

ETH-Bibliothek Zürich, E-Periodica, <https://www.e-periodica.ch>

Plagioclase Determination through Measurement of the Extinction Angles in Sections Normal to (010) and (001)

By *Paolo Bruni* (Zürich)*)

With 14 figures

Abstract

On the basis of available optical data of low-T and high-T plagioclases (BURRI et al., 1967), a proposal is made for a refinement and extension of the classical method of An-content determination by means of extinction angles. Determination diagrams are given for twin laws with composition plane (010) and (001), which do not depend on a specific 2V curve.

FOREWORD

It may be useful to summarize here some general operations.

Distinction between composition planes (010) and (001)

Employing the universal stage, place the composition plane in a vertical position along N-S. Rotate the microscope stage 45° so that the zone axis is parallel to n_γ of the gypsum plate. Insert the plate. If, by rotating on the E-W axis, the interference colors rise, the composition plane is (010); if the colors both rise and fall, the composition plane is either (001) or the rhombic section (RITTMANN, 1929).

This criterion does not work for very calcic plagioclases, as their optic-axes plane is oriented in an unsuitable way.

Distinction between the vertical and horizontal twin axis

When the twin axis is vertical the two individuals show the same birefringence and appear equally illuminated; by rotating the microscope stage they

*) Institut für Kristallographie und Petrographie, ETH-Zentrum, CH-8092 Zürich.

remain indistinguishable, because the rotation axis is coincident with the twin axis and with the direction of observation.

When the twin axis is horizontal there are only two positions in which the two individuals show the same birefringence and hence are illuminated to the same extent, namely those in which the twin axis is located in the vibration planes of polarizer and analyzer. By rotating around the twin axis the structure of the twin complex cannot be seen.

*Identification of the twin laws by means of the extinction angles
of the twinned individuals*

In the following, individual 1 of figure 1 will be called *original* (individual) and individual 2 *twin* (individual). The figures are schematic, the contact planes

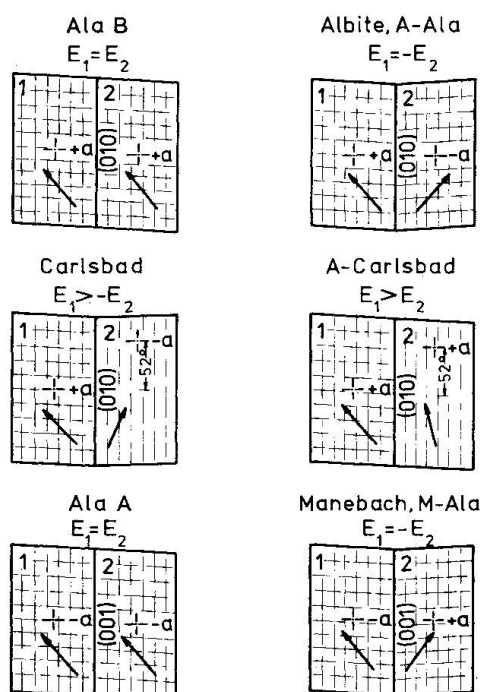


Fig. 1. Extinction relations for several twin laws. Sections \perp a-axis of the original individual.

are vertical and located N-S, axis a of the original individual is normal to the plane of the figure, $+b$ is to the right, and the arrows show the directions of the extinction angles.

- a) Ala B: $E_1 = E_2$, the twin axis is normal to the plane of the figure.
- b) Albite and Albite-Ala: $E_1 = -E_2$, the twin axis of the Albite law lies in the plane of the figure along E-W; the twin axis of the Albite-Ala law lies in the plane of the figure and along N-S.
- c) Carlsbad: $E_1 > -E_2$, by rotation of $\sim 64^\circ$ clockwise around the E-W axis, the twin axis becomes vertical and $E_1 = E_2$; by rotation of $\sim 26^\circ$ counter-clockwise, the twin axis becomes horizontal and $E_1 = -E_2$.

- d) Albite-Carlsbad: $E_1 > E_2$, by rotation of $\sim 26^\circ$ counterclockwise around the E-W axis, the twin axis becomes vertical and $E_1 = E_2$.
- e) Ala A: $E_1 = E_2$, the twin axis is normal to the plane of the figure.
- f) Manebach and Manebach-Ala: $E_1 = -E_2$, the twin axis of the Manebach law lies in the plane of the figure and E-W; the twin axis of the Manebach-Ala law lies in the plane of the figure and N-S.

Because of the near-coincidence of the twin axes, the Manebach-Pericline law cannot be distinguished from the Ala A law within the precision limits attainable with the aid of the universal stage. For the same reasons the Acline law cannot be distinguished from the Manebach-Ala law. In the low-T plagioclase series with An content around 43%, $\gamma = 90^\circ$; hence the twin axes of the Manebach-Pericline and Ala A laws coincide perfectly, as well those of the Acline and Manebach-Ala laws.

Determination of the extinction angles

In order to give an unambiguous sign to the angular measurements, the following convention has been adopted (fig. 2): the extinction directions to be found in a clockwise sense with respect to the reference trace (N-S) will determine positive extinction angles and vice versa.

The initial data consist of the Becke coordinates (λ^* , φ^*) for the optical axes of the original individual with the following orientation:

curves for $n'_\alpha \wedge (010)$: the c-axis is vertical, and its positive part points towards the observer, $+b$ is to the right;

curves for $n'_\alpha \wedge (001)$: the a-axis is vertical and its negative part points towards the observer, $+c$ is to the right.

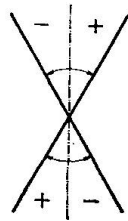
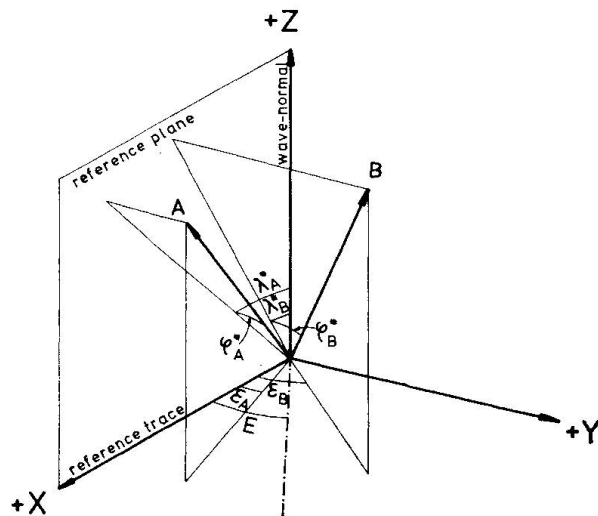


Fig. 2. Sign of the angular measurements.

Fig. 3. Extinction direction in the BECKE coordinate system. A, B: poles of the optical axes.



From those positions the crystal has been made to rotate counterclockwise around the E-W axis at 1° intervals up to 90° : for any explicit rotation degree the extinction angles have been calculated. Furthermore, for any twin law, the extinction angles of the twin individual have been calculated. This rotation is characterized by positive λ values. Subsequently, starting again from the same initial position, a clockwise rotation has been made in the same manner as for the first case. The latter rotation is characterized by negative λ values. Hence $\lambda = 0$ when the twin axis is vertical.

The projection of the optical axes on the plane normal to the wave-normal forme ϵ_A and ϵ_B angles with the reference trace (fig. 3):

$$\epsilon_A = \arctan \frac{\tan \varphi_A^*}{\sin(\lambda_A^* + \lambda)}, \quad \epsilon_B = \arctan \frac{\tan \varphi_B^*}{\sin(\lambda_B^* + \lambda)}.$$

The extinction angle is: $E = (\epsilon_A + \epsilon_B)/2$.

The extinction angles with respect to n'_γ are complementary and of opposite sign.

Even in plagioclase in a well-defined thermal state, $2V$ is not a characteristic constant depending on composition; rather, it is a parameter which may vary more or less widely.

Consideration of this variation in the n_α, n_γ plane means an adoption of two degrees of freedom for $2V$; consequently its value will not be determined by a single curve but rather by a family of curves and the $\%An$ will not be given by a point on a curve, but by a curve in the plane.

For any initial value of $2V$, a variation from -10° to $+10^\circ$, at 2° intervals, has been considered. By means of the newly obtained extinction angles all the diagrams of this work have been drawn. The extinction angles of the original individual are recorded in the ordinates, and those of the twin in the abscissae.

Points with the same $\%An$ are united by iso-An curves (thick lines) and points with the same $2V_\gamma$ by iso- $2V$ curves (thin lines). On both curves the corresponding $\%An$ and $2V_\gamma$ values are recorded. Therefore a point on the diagrams can be determined by three pairs of parameters: (E_1, E_2) , $(E_1, 2V)$, $(E_2, 2V)$, where, of course, the determination of (E_1, E_2) is the easiest.

The complex laws give curves symmetrical to those of the corresponding parallel laws, about the ordinate axis. For all the diagrams λ is positive. If it is not possible to determine the sign of λ , the same uncertainty will affect E_1 and E_2 too.

The more reliable diagrams are those in which the iso-An curves are widely spaced from each other and slightly inclined relative to the iso- $2V$ curves. On the diagrams $\%An$ at 5% -intervals are recorded: intermediate values are obtained by interpolation. The λ values were chosen in such a way as to give the most reliable and useful diagrams.

Errors affecting the measurements

The systematic errors, which are related to the skill of the observer and to the quality of the instrument, include:

1. error of N-S alignment of the reference trace;
2. error of verticality in the orientation of the reference plane;
3. error of λ .

If we consider a parallel-law twin, such as Carlsbad, and suppose that each of its individuals is in turn twinned according to the Albite law (fig. 4), error 1

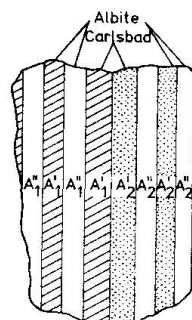


Fig. 4. Carlsbad twin with both individuals exhibiting Albite twin lamellae.

can be eliminated and 2 largely compensated by determining the extinction angle of the original individual (E_1) and of its twin (E_2) in the following way:

$$E_1 = \frac{E_{A_1'} - E_{A_1''}}{2}, \quad E_2 = \frac{E_{A_2'} - E_{A_2''}}{2}.$$

E_{01} , E_{02} being the extinction angles calculated with a vertical reference plane, $|E_{01} - E_1|$ and $|E_{02} - E_2|$ are so small that even for a $\pm 3^\circ$ tilt of the reference plane they turn out to be less than 0.1° for any An in all determination diagrams shown in this work.

An example will make clear what is meant by making use of a normal law: high-T, 60%An, Carlsbad + polysynthetic Albite, $\lambda = 30$, tilt = $+3^\circ$.

$$E_1 = \frac{29.7156^\circ - (-34.3769^\circ)}{2} = 32.0462^\circ,$$

$$E_2 = \frac{-9.9057^\circ - 5.2319^\circ}{2} = -7.5688^\circ,$$

$$E_{01} = 31.9484^\circ, \quad E_{02} = -7.5260^\circ,$$

$$|E_{01} - E_1| = 0.0978^\circ, \quad |E_{02} - E_2| = 0.0428^\circ.$$

Error 3 is largely compensated by determining (if possible) the extinction angles in the following way:

$$E_1 = \frac{E_1(\lambda) + E_2(-\lambda)}{2}, \quad E_2 = \frac{E_2(\lambda) + E_1(-\lambda)}{2}.$$

An example: high-T, 40%An, Carlsbad, $\lambda = 30 (\pm 2^\circ)$, namely actual $\lambda = 28$ or 32.

$$E_1 = \frac{20.9191^\circ + 19.1102^\circ}{2} = 20.0146^\circ,$$

$$E_2 = \frac{-1.5884^\circ - 0.6354^\circ}{2} = -1.1119^\circ.$$

The values calculated for $\lambda = 30$ are:

$$E_1 = 20.0253^\circ, \quad E_2 = -1.1131^\circ.$$

Corresponding errors: 0.0107° and 0.0012° .

Compensation relations for errors 1, 2, 3:

$$E_1 = \frac{E_{A_1'}(\lambda) - E_{A_1''}(\lambda)}{4} + \frac{E_{A_2'}(-\lambda) - E_{A_2''}(-\lambda)}{4},$$

$$E_2 = \frac{E_{A_2'}(\lambda) - E_{A_2''}(\lambda)}{4} + \frac{E_{A_1'}(-\lambda) - E_{A_1''}(-\lambda)}{4}.$$

Acknowledgements

The computations were performed on the CDC 6400 at the Zürich ETH Computer Center. The author wishes to thank Dr. A. ALBERTI, Prof. Dr. C. BURRI, Prof. Dr. W. G. ERNST, M. GYSEL-FRANGIPANE and PD Dr. R. SCHMID.

Diagrams

Legend: E_1 : extinction angle of the original individual;
 E_2 : extinction angle of the twin individual;
 λ : angle between twin axis and observation direction;
 thick lines: %An;
 thin lines: $2V_\gamma$.

The complex laws give curves symmetrical to those of the corresponding parallel laws, about the ordinate axis.

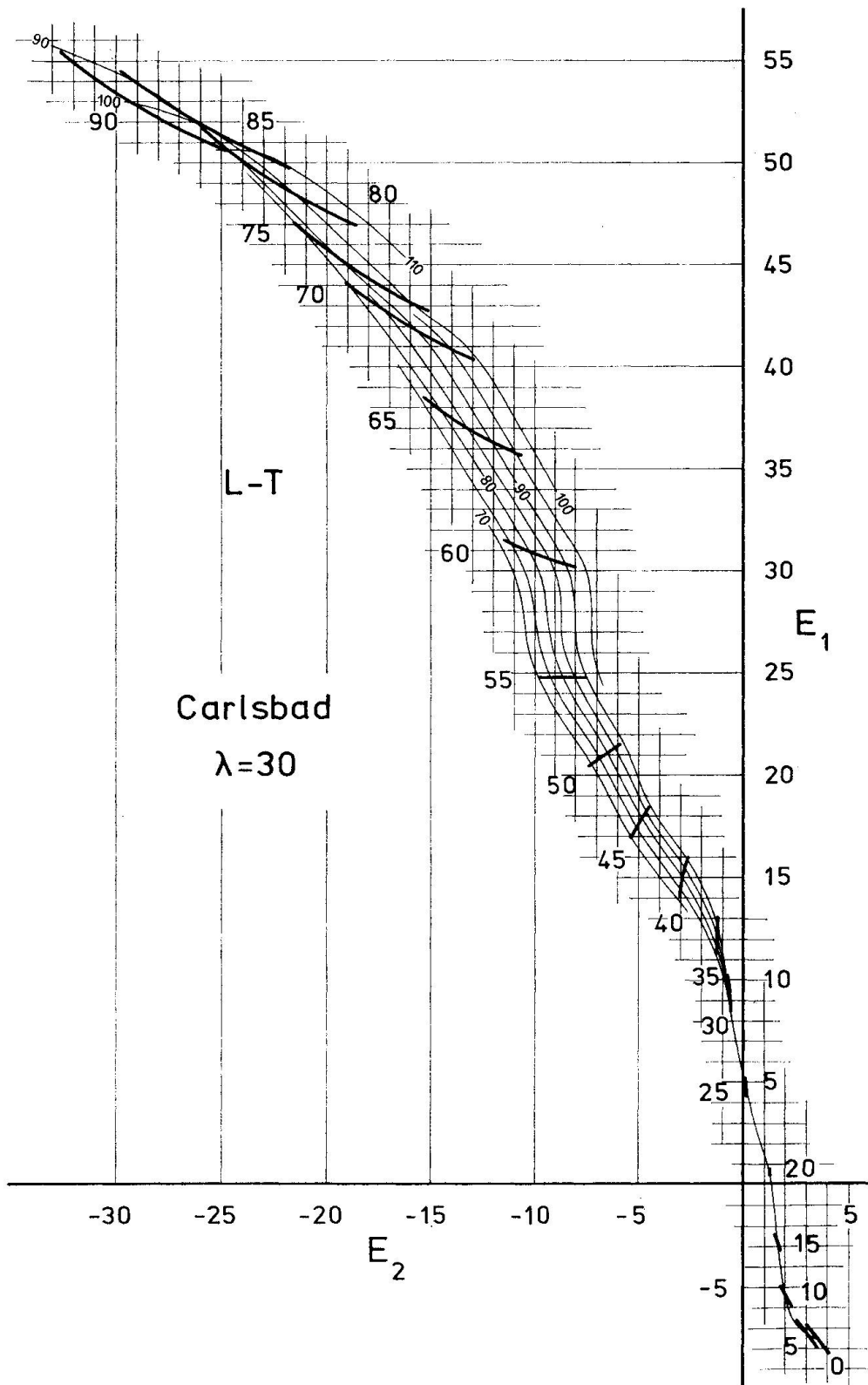


Fig. 5. Carlsbad and Albite-Carlsbad, $\lambda = 30$, low-T.

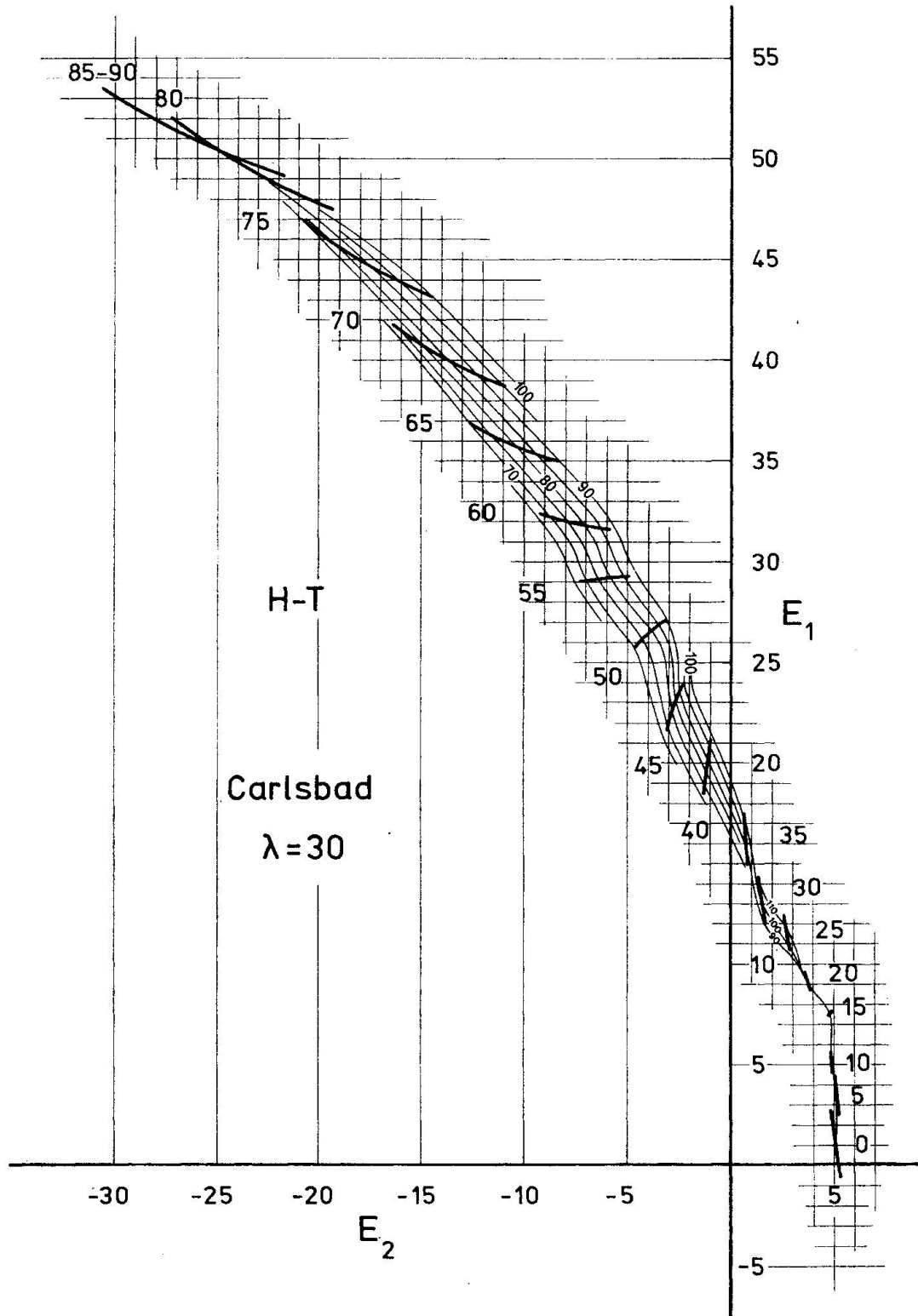


Fig. 6. Carlsbad and Albite-Carlsbad, $\lambda = 30$, high-T.

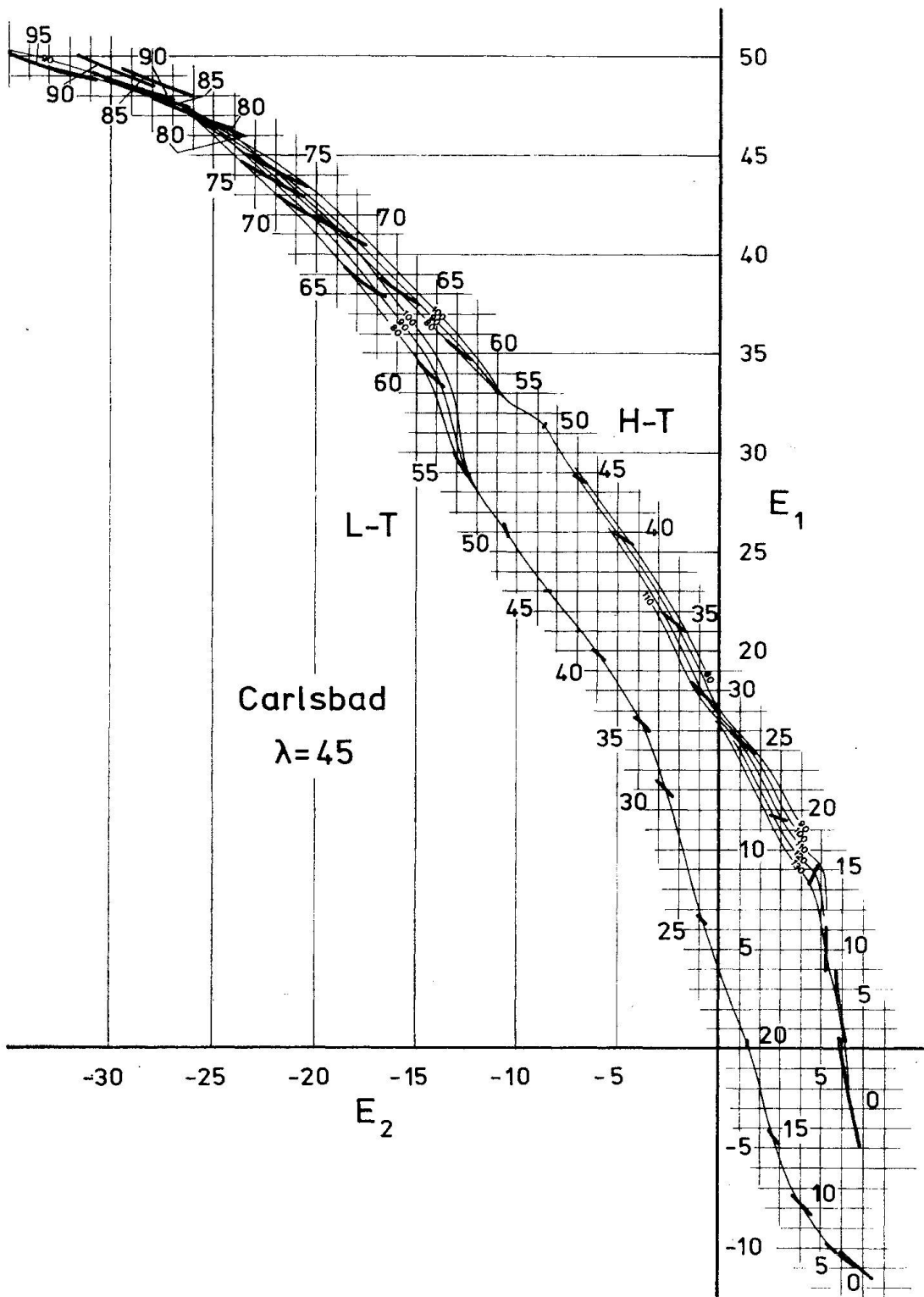


Fig. 7. Carlsbad and Albite-Carlsbad, $\lambda = 45$, low-T and high-T.

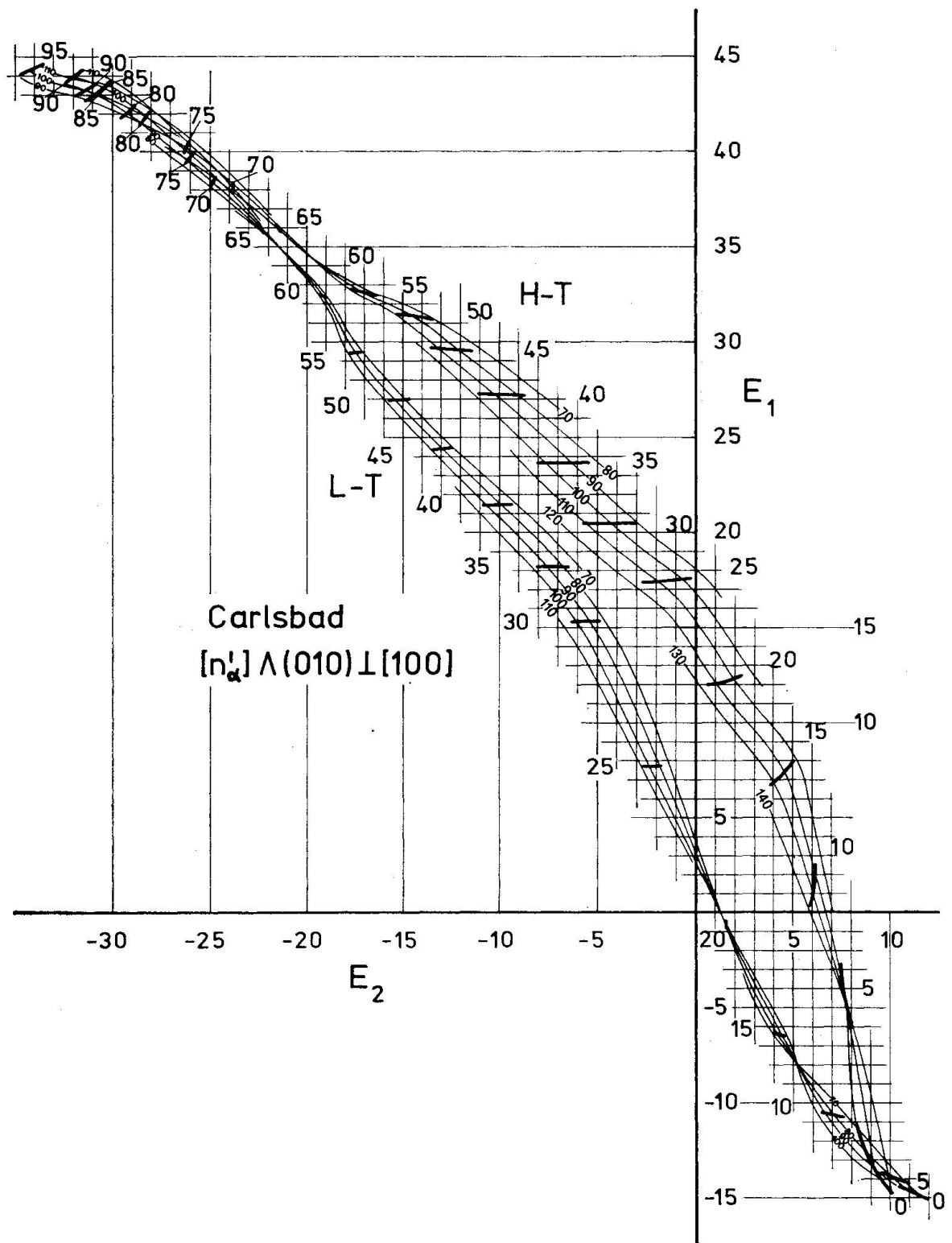


Fig. 8. Carlsbad and Albite-Carlsbad, $n'_\alpha \wedge (010) \perp [100]$, low-T and high-T.

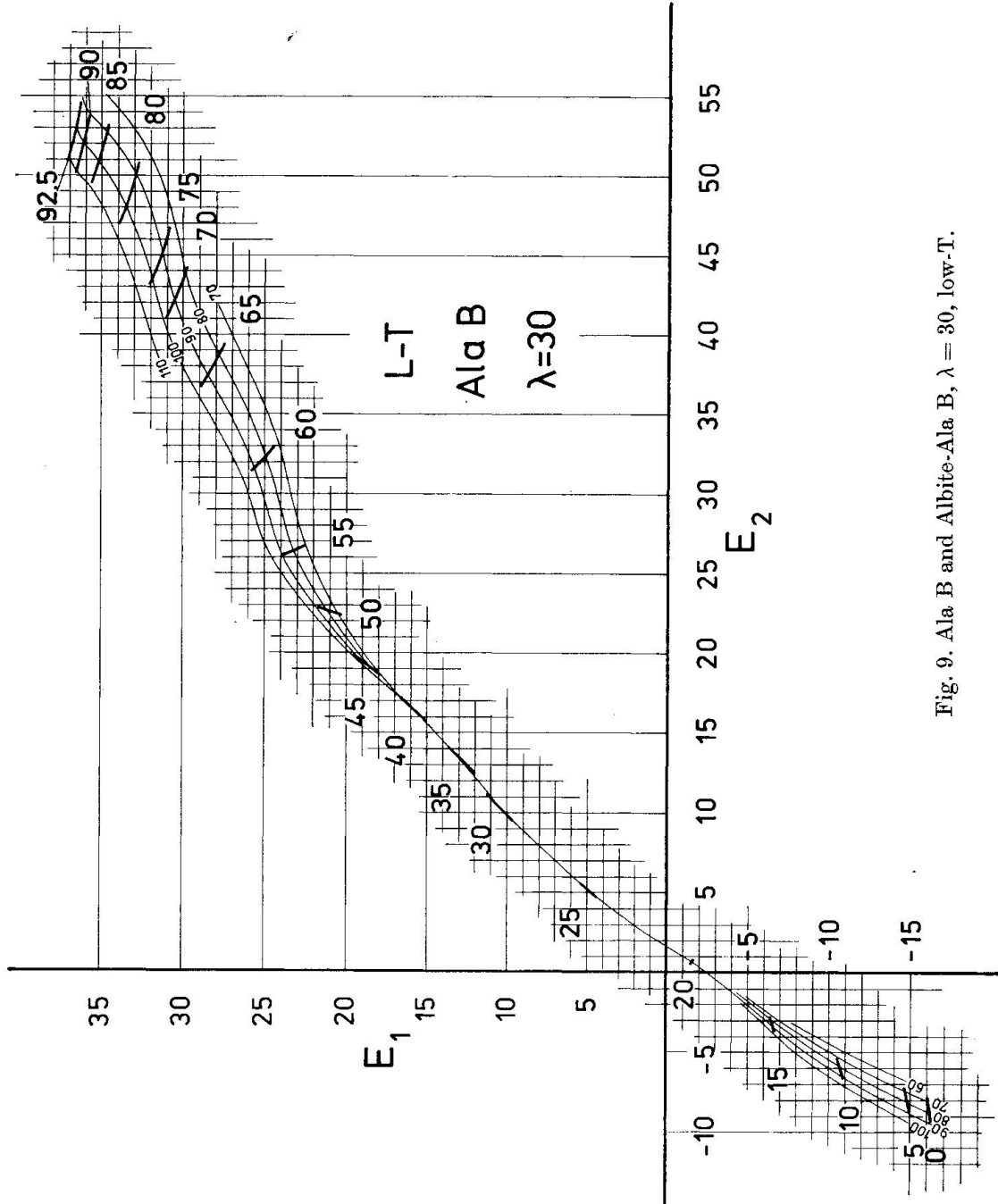
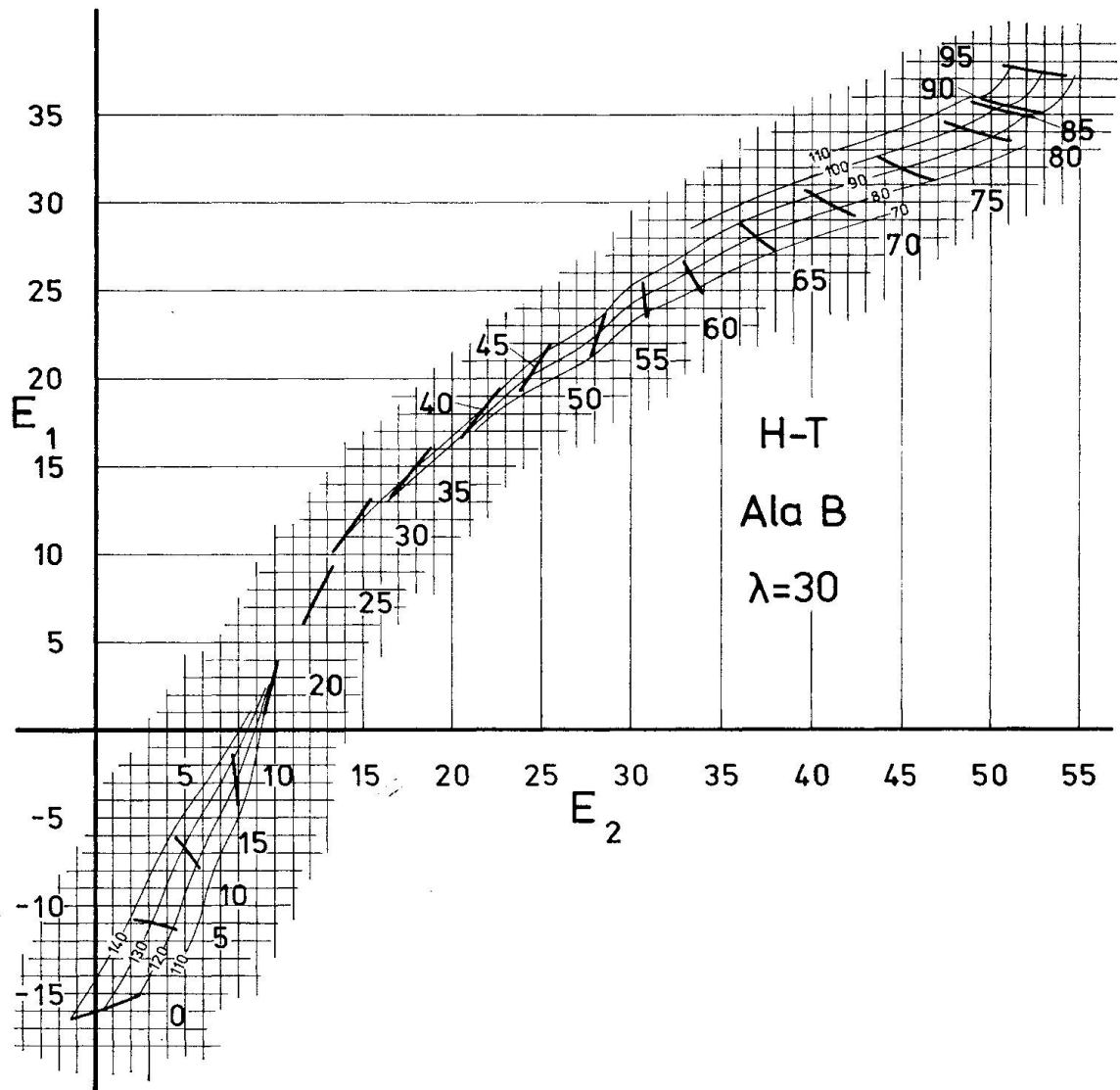


Fig. 9. Alα B and Albite-Alα B, $\lambda = 30$, low-T.

Fig. 10. Ala B and Albite-Ala B, $\lambda = 30$, high-T.

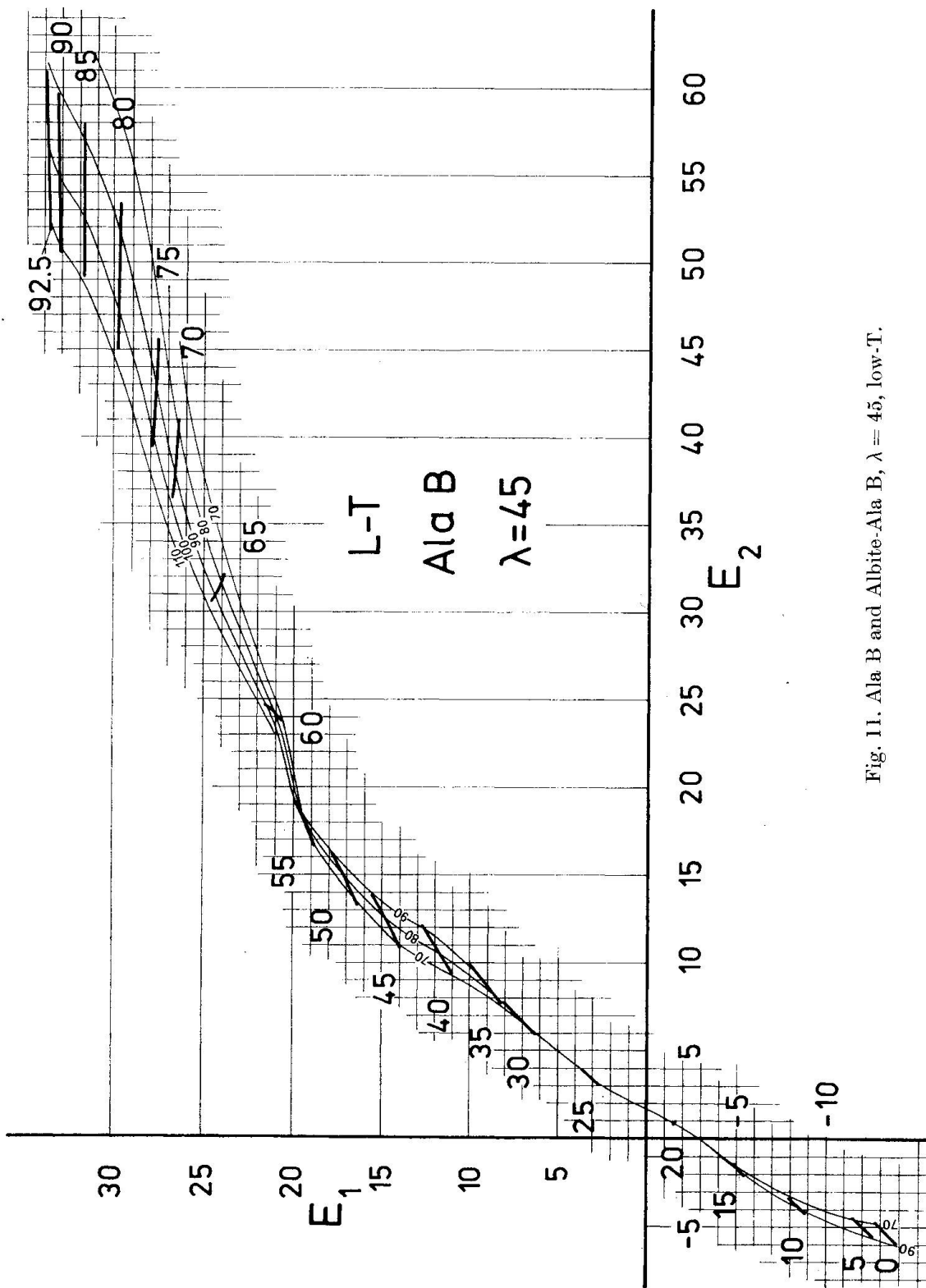


Fig. 11. Ala B and Albite-Ala B, $\lambda = 45$, low-T.

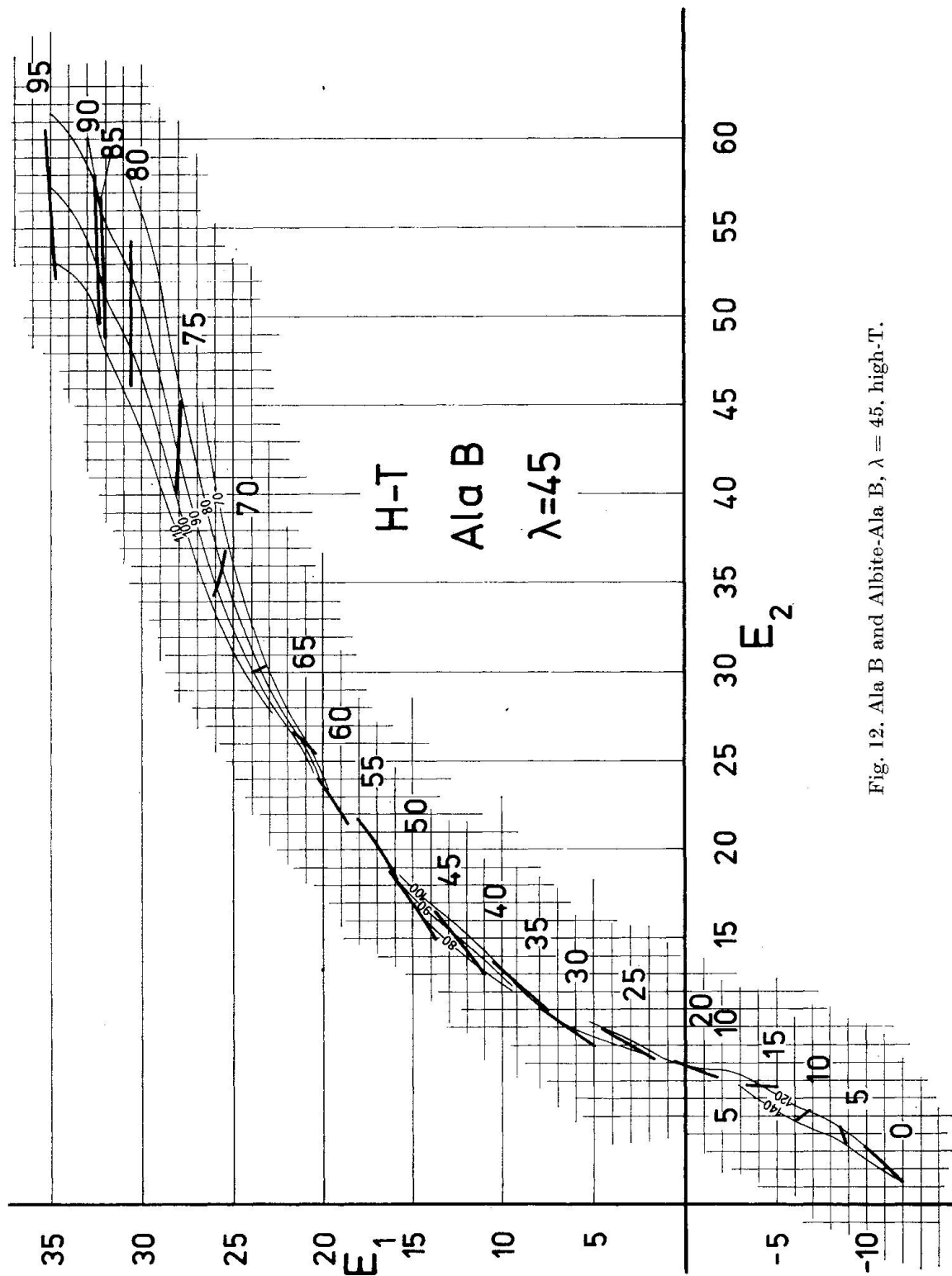


Fig. 12. Ala B and Albite-Ala B, $\lambda = 45$, high-T.

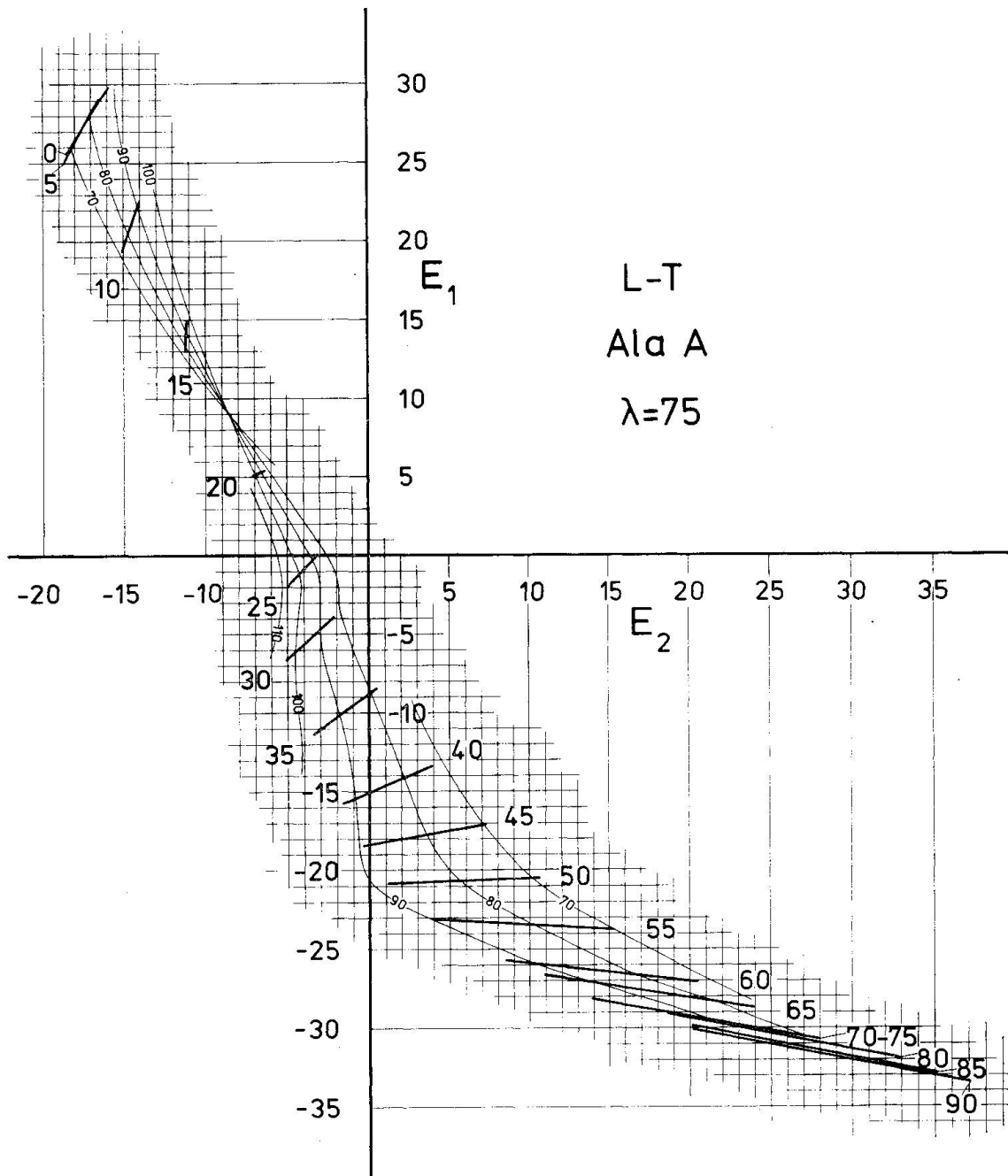


Fig. 13. Ala A and Manebach-Ala A, $\lambda = 75$, low-T.

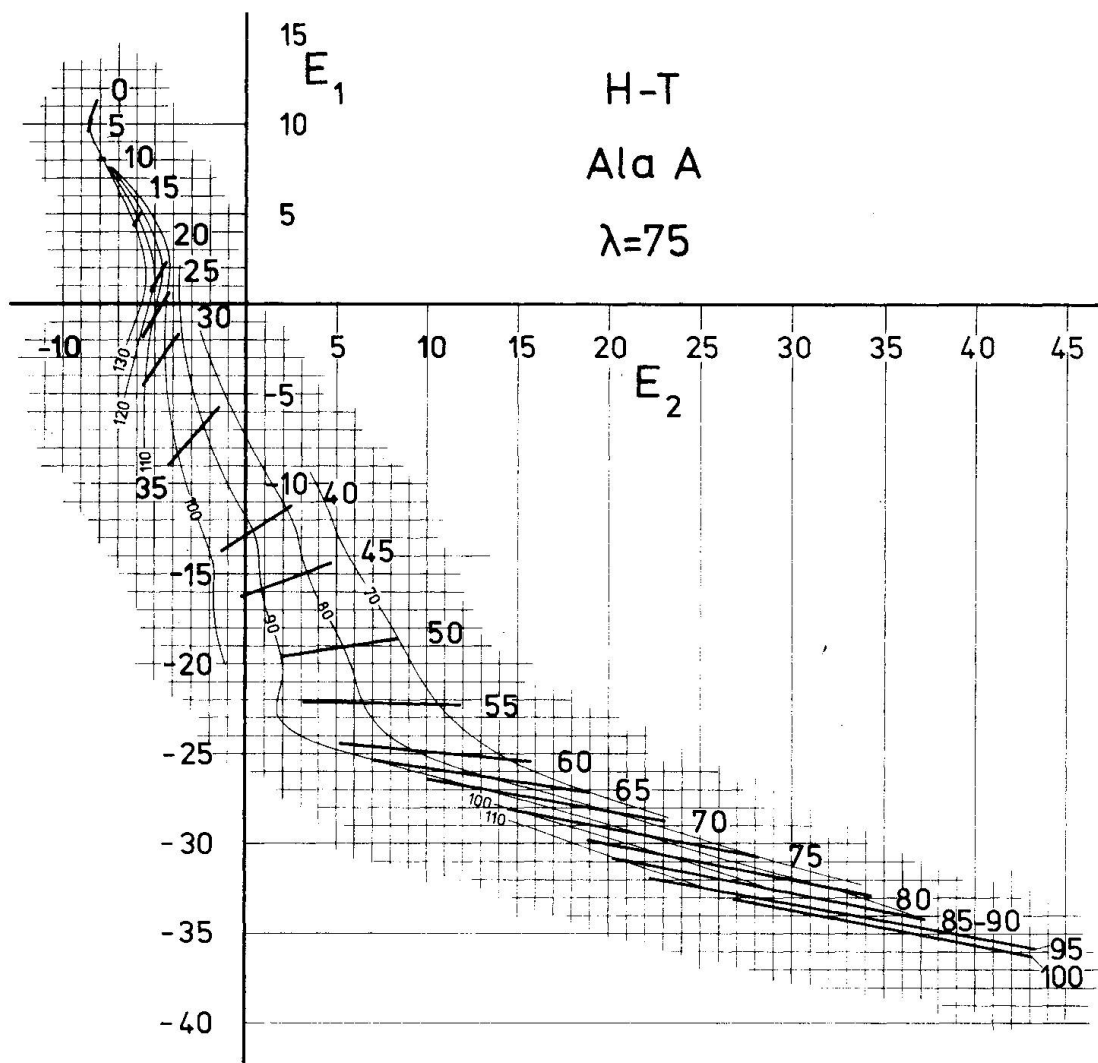


Fig. 14. Ala A and Manebach-Ala A, $\lambda = 75$ high-T.

Bibliography

- BURRI, C., R. L. PARKER und E. WENK (1967): Die optische Orientierung der Plagioklase. Basel, Birkhäuser.
- FRANZINI, M. (1965): Sulla determinazione della composizione e dello stato termico dei plagioclasidi geminati Albite-Karlsbad. Atti della Soc. Tosc. Sc. Nat. Serie A, Vol. LXXII.
- RITTMANN, A. (1929): Die Zonenmethode. SMPM 9, 1-46.
- TOBI, A. C. (1975): Optical determination of the An content of plagioclases twinned by Carlsbad-law: a revised chart. Am. Jour. Sci., Vol. 275, 731-736.

Manuscript received September 26, 1975.